Available online at www.sciencedirect.com
SCIENCE DIRECT®
Journal of Catalysis 231 (2005) 292–299
JOURNAL OF CATALYSIS
www.elsevier.com/locate/jcat

Electrophilic property of O_3^- photoformed on isolated Ti species in silica promoting alkene epoxidation

Chizu Murata [a,1], Tadashi Hattori [a], Hisao Yoshida [b,*]

[a] *Department of Applied Chemistry, Graduate School of Engineering, Nagoya University, Nagoya 464-8603, Japan*
[b] *Division of Environmental Research, EcoTopia Science Institute, Nagoya University, Nagoya 464-8603, Japan*

Received 5 October 2004; revised 18 December 2004; accepted 13 January 2005

Available online 19 March 2005

Abstract

We previously reported that photoformed O_3^- species on highly dispersed titanium oxide species are the active oxygen species for the epoxidation of propene. In the present study, it was found that this epoxidation system could be extended to other light alkenes such as ethene and butene, and the electronic structure of the O_3^- species and reaction mechanism of the insertion of atomic oxygen into the C=C bond in olefin were revealed. An isotope-labeled reaction test with $^{18}O_2$ and ESR measurement with $^{17}O_2$ clarified the following mechanism: the O_3^- species is generated by the reaction between an O_2 molecule and a photoformed hole center on lattice oxygen (O_L^-), and the photoformed hole in the O_3^- moves from the lattice oxygen (O_L^-) to the O_2 moiety derived from molecular oxygen. The O_3^- species can be also described as a surface complex of O_L^{2-} (electronic neutral) and adsorbed O_2^+. This electron-deficient oxygen moiety derived from molecular oxygen could preferably react with the electron rich part of alkene, the C=C bond, to produce epoxide.

Keywords: Electrophilic oxygen species; Molecular oxygen; Photocatalyst; Propene epoxidation; Titania–silica

1. Introduction

The epoxidation of propene is an important catalytic reaction in the chemical industry. Despite its importance, there is still no direct epoxidation process by molecular oxygen for the preparation of propene oxide (PO) [1,2]. Although the Ag/Al_2O_3-catalyzed gas phase epoxidation of ethylene with molecular oxygen is one of the most successful examples of heterogeneous catalysis [1,3], this process has not been applied to propene epoxidation [3]. The existence of allylic C–H bonds, which are much more subject to dehydrogenation than the vinyl C–H bonds in ethylene, prevents the high selectivity for PO. Although several groups have reported the direct epoxidation of propene with the use of only molecular oxygen in heterogeneous catalytic systems [3–10] and noncatalytic radical reaction systems [11,12], the industrial process of propene epoxidation with only molecular oxygen has not been developed. A novel concept, how to activate molecular oxygen, is required for a breakthrough.

Photosystems could be proposed as a potential approach to epoxidation by molecular oxygen, although the activity would still be low [13]. The epoxidation of higher alkenes in the liquid phase with photocatalyst has been reported for both heterogeneous [14–16] and homogeneous [17–19] systems. As for the photoepoxidation of propene, several systems using TiO_2 [20], Ba-Y type zeolite [21–23], and various silica-supported metal oxides [24–36] have been reported. If the active oxygen species and detailed reaction mechanism are revealed, the concept might be applied to the catalyst design, even in general thermal epoxidation. However, the active oxygen species have not been examined in these photosystems. We disclosed that the highly dispersed titanium oxide species on silica catalyzed photoepoxidation of propene with molecular oxygen, with high yield and selectivity [24–27]. ESR measurement and the reaction of the

* Corresponding author. Fax: +81 52 789 5849.
E-mail address: h-yoshida@esi.nagoya-u.ac.jp (H. Yoshida).
[1] Present address: JGC Corporation, 2205, Narita-cho, Oarai-machi, Higashiibaraki-gun, Ibaraki Pref., 311-1313, Japan.

0021-9517/$ – see front matter
doi:10.1016/j.jcat.2005.01.012

active oxygen species with propene indicated that the photoformed T-type O_3^-, which is produced by the reaction of photoformed O_L^- (a hole center on lattice oxygen) with the O_2 molecule, was the active oxygen species for the photoepoxidation of propene [24]. However, it was not enough to reveal the property of the O_3^- and the detailed reaction mechanism.

Generally, it is accepted that the electrophilic oxygen species are effective for the epoxidation of alkenes [1,2,37,38]. Several active oxygen species have been proposed, such as atomic oxygen at ground state, $O(^3P)$ [39–41], electrophilic atomic oxygen species on Ag/Al_2O_3 in epoxidation of ethylene by molecular oxygen [1], and peroxometal or oxometal intermediates in metal-catalyzed epoxidation with hydroperoxide reagents [42–45]. It is well known that cytochrome P-450, a monooxygenase, generates the electrophilic oxygen species from O_2 with a reducing agent to catalyze the epoxidation of alkenes and hydroxylation of alkanes and aromatics [46]. However, it has not been proposed that the photoformed O_3^- is the electrophilic oxygen species, except for our previous study [24]. It is valuable to reveal the property of the O_3^- and how the O_3^- reacts with propene to produce epoxide.

In the present study, we investigated the electronic structure of the O_3^- species and the detailed mechanism of propene photoepoxidation by using various alkenes (C2–C4) photoepoxidation tests, isotopic experiments with $^{18}O_2$, and ESR with ^{17}O-enriched oxygen. It was asked why the photoformed O_3^- species on highly dispersed titanium oxide species could promote propene epoxidation.

2. Experimental

A TiO_2–SiO_2 catalyst of low Ti content (Ti content 0.34 mol%; mol% Ti $= N_{Ti}/(N_{Ti} + N_{Si}) \times 100$) was prepared by the sol–gel method, consisting of a two-stage hydrolysis procedure [47]. A mixture of tetraethoxyorthosilicate (TEOS), ethanol, distilled water, and nitric acid was stirred at 353 K for 3 h to hydrolyze TEOS partially, and the sol obtained was cooled to room temperature. A 2-propanol solution of titanium isopropoxide was added to the sol and stirred for 2 h. Then an aqueous nitric acid solution was added to the sol and stirred until the gelation was completed. The gel was dried and calcined at 773 K. The BET surface area of the sample was 423 $m^2\,g^{-1}$. It was confirmed that this sample predominantly contained the isolated tetrahedral Ti species, from the diffuse reflectance UV spectrum [24–26].

Before each reaction test and spectroscopic measurement, the sample was treated with 100 Torr oxygen (1 Torr = 133.3 $N\,m^{-2}$) at 773 K for 1 h, followed by evacuation at 673 K for 1 h. The photooxidation of alkenes was performed in a manner similar to that previously described [24,25]. When $^{18}O_2$ (ICON, 99%) was employed for the photooxidation of propene, the products were analyzed by GC-FID and GC-MS. The total amounts of ^{18}O-compound and ^{16}O-compound were determined by GC-FID. The ratio of ^{18}O-compound to ^{16}O-compound was calculated from the GC-MS peak area. The monitored mass numbers were $m/e =$ 58, 60 for PO, $m/e = 44$, 46 for ethanal, and $m/e = 56$, 58 for acrolein, respectively. We calculated the real area of the ^{16}O-compound by subtracting the area of the ^{18}O-compound fragment from the observed mass peak area.

Photoinduced oxygen isotopic exchange reaction between lattice oxygen (^{16}O) in the catalyst and molecular oxygen ($^{18}O_2$) was performed with a conventional closed circulating system (221 cm^3) connected to a mass spectrometer. $^{18}O_2$ (0.2 Torr) was admitted to the pretreated catalyst (1.0 g), and then the catalyst was irradiated with a 200-W Xe lamp. The ratio of the concentration of $^{16}O\,^{18}O$ molecules ($m/e = 34$) to $^{18}O_2$ molecules ($m/e = 36$) was measured with the mass spectrometer.

ESR spectra were measured at 77 K with an X-band JEOL JES-TE200 spectrometer at a microwave power level of 1.0 mW, at which microwave power saturation of the signals did not occur. The sample was irradiated with a 500-W ultrahigh-pressure Hg lamp at 77 K. The magnetic field was calibrated with a JEOL NMR field meter ES-FC5.

3. Results

3.1. Photoepoxidation of various alkenes

Table 1 shows the results of the photoepoxidation of various alkenes (ethene, propene, 1-butene, *cis*-2-butene, *trans*-2-butene) over the TiO_2–SiO_2 catalyst. The main products from these alkenes were epoxides, CC cleavage products, allylic oxidation products, and CO_x. The selectivity for each epoxide was around 45–67%; alkenes with allylic C–H bonds exhibited higher selectivity for epoxides than ethylene with no allylic C–H bonds. It was confirmed that this photoepoxidation system is generally available for light alkenes, even if the alkene has allylic C–H bonds.

The yield of epoxide increased in the following order: $C_2H_4 < C_3H_6 <$ 1-$C_4H_8 <$ *cis*-2-$C_4H_8 <$ *trans*-2-C_4H_8. This order roughly agreed with the electron density on the C=C bond in alkene, which depends on the substituent groups in alkene. Epoxides would be formed by the reaction of alkenes with the O_3^- [24]. Therefore, this result proved that the O_3^- has an electrophilic nature in common with previously reported active oxygen species in these epoxidation systems [37–46]. Yields of CC cleavage products and allylic oxidation products also increased with increasing electron density of the C=C bond, because the photoactivated O_L^- species, a hole trapping lattice oxygen, should also be electrophilic, and the alkene reacts with it directly, as proposed in the previous study [24].

cis-2-Butene and *trans*-2-butene produced both *trans*-2,3-epoxybutane and *cis*-2,3-epoxybutane (Table 1). Thus the possibility of the isomerization of 2-butenes and 2,3-epoxybutenes in the photooxidation was examined. When

Table 1
Results of photoepoxidation of various alkenes by molecular oxygen over the TiO_2–SiO_2 catalyst

Substrate	Conversion to oxygenate products[a] (%)	Yield of epoxides (%)	Selectivity to epoxides (%)	Yield (%)
C_2H_4	1.8	0.8	45	**Ethylene oxide (0.8)**, ethanal (0.3), formaldehyde (0.1), CO_x[b] (0.5)
C_3H_6	10.1	5.7	55	**Propene oxide (5.7)**, propanal (0.2), acetone (0.9), ethanal (1.3), acrolein (0.9), CO_x (0.8)
1-C_4H_8	11.6	6.8	55	**1,2-Epoxybutane (6.8)**, butanone (0.5), butanal (0.6), ethanal (1.4), propanal (0.4), methyl vinyl ketone (0.5), crotonaldehyde (0.3), CO_x (1.0)
cis-2-C_4H_8	18.4	12.5	67	***trans*-2,3-Epoxybutane (6.0), *cis*-2,3-epoxybutane (6.5)**, butanone (0.1), ethanal (3.4), methyl vinyl ketone (0.7), crotonaldehyde (0.8), CO_x (0.8), *trans*-2-C_4H_8 (4.4), 1-C_4H_8 (0.5)
trans-2-C_4H_8	24.4	16.4	66	***trans*-2,3-Epoxybutane (12.8), *cis*-2,3-epoxybutane (3.6)**, butanone (0.8), butanal (0.2), ethanal (4.2), methyl vinyl ketone (0.9), crotonaldehyde (1.2), CO_x (0.8), *cis*-2-C_4H_8 (0.6), 1-C_4H_8 (0.7)

Catalyst 0.2 g, alkene 100 μmol, O_2 100 μmol, irradiation time 2 h.
[a] Conversion shows the sum of the oxygenate products. Although the isomerization of *cis*-2-butene was appreciable, the hydrocarbon products were not taken into account here.
[b] CO_x is $CO + CO_2$.

Table 2
Results of photoisomerization of 2-butene over the TiO_2–SiO_2 catalyst

Reactant	Yield (%)			
	Ethanal	1-Butene	*trans*-2-C_4H_8	*cis*-2-C_4H_8
cis-2-C_4H_8	0.2	4.3	7.5	–
trans-2-C_4H_8	0.0	2.3	–	0.0

Catalyst 0.2 g, 2-butene 100 μmol, irradiation time 2 h.

the photoisomerization of 2-butenes was examined in the absence of O_2 (Table 2), *cis*-2-butene was isomerized into *trans*-2-butene and 1-butene. On the other hand, *trans*-2-butene was isomerized into 1-butene, but not into *cis*-2-butene at all. Table 3 lists the results of the isomerization of *cis*-2,3-epoxybutane and *trans*-2,3-epoxybutane. They were scarcely isomerized in the presence of O_2 under photoirradiation. If the photoepoxidation occurred stereospecifically, *cis*-2,3-epoxybutane cannot be formed from *trans*-2-butene. However, *trans*-2-butene converted to both *cis*-2,3-epoxybutane and *trans*-2,3-epoxybutane in the photoepoxidation. This means that the photoepoxidation proceeds nonstereospecifically. The photoepoxidation might proceed through the biradical-like intermediate in a manner similar to that of the epoxidation with O(^{3}P) [39–41], UV-irradiated NO_2 [48–50], and vanadium hydroperoxo species [51].

3.2. Isotopic studies of the oxygen atom insertion mechanism with $^{18}O_2$

Fig. 1 shows the result of the oxygen isotopic exchange reaction between the lattice oxygen (^{16}O) and molecular oxygen ($^{18}O_2$) over the catalyst. The exchange reaction did not occur in the dark. The photoirradiation brought about the exchange reaction, and the reaction stopped when the light was turned off. When the light was turned on again, the exchange reaction proceeded (not shown). These results indicate that a surface oxygen complex would be derived from both molecular oxygen and the lattice oxygen upon photoirradiation. In our previous study, it was found that O_3^- and O_2^- were generated over the TiO_2–SiO_2 catalyst in the presence of O_2 by photoirradiation [24]. The O_3^- originated from O_2 and O_L^- (a hole trapping lattice oxygen), and O_2^- is made of O_2 and an electron. When the light was turned off at room temperature, the O_3^- immediately disappeared, and O_2^- remained [24]. From these aspects and the present results, it is suggested that the oxygen isotopic exchange reaction proceeds through the O_3^- intermediate over the catalyst in the absence of propene. This agrees with the reported phenomena on TiO_2 [52] and porous Vycor glass (PVG) [53], where the photoinduced oxygen isotopic exchange reaction proceeded through the O_3^- intermediate.

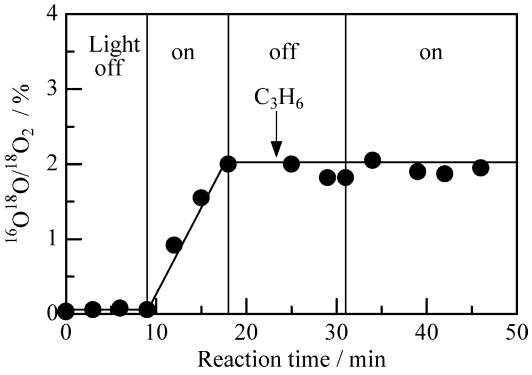

Fig. 1. Variation of the ratio of $^{16}O\,^{18}O$ molecules ($m/e = 34$) to $^{18}O_2$ molecules ($m/e = 36$) in photoinduced oxygen isotopic exchange reaction over the TiO_2–SiO_2 catalyst (0.5 g) in the presence of $^{18}O_2$ (0.2 Torr). At the time indicated by arrow, propene (0.1 Torr) was introduced.

As shown in Fig. 1, the addition of a small amount of propene completely inhibited this exchange reaction, even under photoirradiation. The O_3^- and O_2^- ESR signals were observed in the presence of O_2 molecules and propene under photoirradiation at 77 K (not shown). We previously suggested that propene reacts with O_3^- to produce PO [24]. In the presence of a O_2 molecule and propene, the O_3^- intermediate certainly exists, but it is too unstable to promote the

Table 3
Results of photoisomerization of 2,3-epoxybutane over the TiO_2–SiO_2 catalyst

Reactant	Products (μmol)							
	trans-EB[a]	*cis*-EB[a]	Butanone	Ethanal	1-C_4H_8	*trans*-2-C_4H_8	*cis*-2-C_4H_8	CO_x
cis-EB[a]	0.1	–	0.3	0.6	0.0	0.0	0.1	0.1
trans-EB[a]	–	0.3	0.2	1.0	0.1	0.0	0.4	0.2

Catalyst 0.2 g, 2,3-epoxybutane 10 μmol, O_2 100 μmol, irradiation time 2 h.
[a] *cis*-EB, *cis*-2,3-epoxybutane; *trans*-EB, *trans*-2,3-epoxybutane.

Table 4
Results of the photoepoxidation of propene over the TiO_2–SiO_2 catalyst using $^{18}O_2$

Catalyst weight (g)	Ti content[a] (μmol)	Time[b] (h)	Conversion (%)	TON	PO selectivity (%)	Yield (%)			^{18}O content (%)		
						PO	Ethanal	Acrolein	PO	Ethanal	Acrolein
0.5	28	1	8.4	0.3	54	4.5	2.4	0.8	98	46	63
0.2	11	14	64.4	5.9	40	25.8	3.7	0.9	97	64	–[c]

Catalyst 0.2 g, C_3H_6 100 μmol, $^{18}O_2$ 200 μmol.
[a] The content of Ti in the catalyst employed in the reaction test.
[b] Irradiation time.
[c] MS peak of both the ^{18}O and ^{16}O compounds could not be observed.

oxygen isotopic exchange reaction. The O_3^- would immediately decompose by the reaction with propene at room temperature, so the oxygen isotopic exchange reaction would be inhibited. In addition, the formation of the O_3^- should be partly inhibited by the reaction of O_L^- with propene to form ethanal or acrolein. A similar inhibition effect on the exchange reaction by the addition of butane or CO was reported in common over TiO_2 or PVG [52,53].

The photoepoxidation of propene with $^{18}O_2$ was carried out over the TiO_2–SiO_2 catalyst (Table 4). Conversion and PO selectivity were similar to those in the reaction with $^{16}O_2$ [24]. As for the main products, such as PO, ethanal, and acrolein, the yield and ^{18}O content are listed in Table 4. It is noteworthy that almost all PO contained ^{18}O at both the initial (TON = 0.3) and later (TON = 5.9) stages of the reaction. On the other hand, approximately a half of ethanal and acrolein contained ^{18}O. The possibility of the oxygen isotopic exchange reaction in the presence of propene was excluded by the result in Fig. 1. Therefore, it was clearly shown that the oxygen atom originating from molecular oxygen (^{18}O) in the O_3^- species was consumed to produce PO, and both the lattice oxygen and molecular oxygen were involved with the production of ethanal and acrolein.

3.3. Structure and electron density of the O_3^-

As described in our previous study [24], when the TiO_2–SiO_2 catalyst was photoirradiated at 77 K in the presence of $^{16}O_2$, O_2^- ($g_{xx} = 2.003$, $g_{yy} = 2.009$, $g_{zz} = 2.025$) [54–57] and T-type O_3^- ($g_\parallel = 2.008$, $g_\perp = 2.002$) [55–57] were observed. When the sample was warmed to room temperature, only the O_2^- signal remained, showing that the O_2^- species are quite stable.

Fig. 2 shows the ESR signals of the TiO_2–SiO_2 sample photoirradiated in the presence of O_2 enriched with ^{17}O (90.4%). The signal at room temperature (Fig. 2b, dotted line) should be the O_2^- signal, judging from ESR with $^{16}O_2$. On this ESR signal, two sets of hyperfine patterns with 6 and 11 lines separated by $A = 7.51$ mT centered at $g = 2.0025$ were observed. These lines would be due to $^{16}O\,^{17}O^-$ and $^{17}O_2^-$, respectively. The ESR parameters ($g_{xx} = 2.0025$, $g_{yy} = 2.0090$, $g_{zz} = 2.0250$, $A_{xx} = 7.51$ mT, $A_{yy} = A_{zz} = 0$ mT) were derived from the signal of O_2^-. Most of these parameters were similar to those of O_2^- on TiO_2/PVG, although two A_{xx} values were observed on these samples [54,55]. The signal at 77 K was estimated to be the superimposition of O_3^- and O_2^- (Fig. 2a, solid line). The four arrows in Fig. 2 point to the obvious difference between the spectrum taken at 77 K and that taken at room temperature. When the signal at room temperature (O_2^-) was subtracted from the signal at 77 K (O_3^- and O_2^-), the signal assigned to O_3^- ($g_1 = 2.0080$, $g_2 \approx 2.003$, $g_3 = 2.0026$, $A_1 \approx A_2 \approx 0$ mT, $A_3 = 7.86$ mT) was obtained (Fig. 2c). The two sets of 6 and 11 lines with a splitting of 7.86 mT would correspond, respectively, to $^{16}O\,^{17}O$ and $^{17}O\,^{17}O$ adsorbed on $^{16}O_L^-$. This indicates that the O_3^- on the catalyst has two equivalent oxygen atoms derived from molecular oxygen; that is, the O_3^- would have the T-type structure.

The hyperfine tensor is resolved into an isotropic part and an anisotropic part in the following form if the unpaired electron is localized in only one p orbital [58,59]:

$$\begin{vmatrix} A_1 & & \\ & A_2 & \\ & & A_3 \end{vmatrix} = a_{\mathrm{iso}} + \begin{vmatrix} -\beta & & \\ & -\beta & \\ & & 2\beta \end{vmatrix}. \quad (1)$$

The terms a_{iso} and 2β in Eq. (1) are, respectively, the isotropic coupling constant and the zz component of the dipolar coupling constant.

The hyperfine constant along g_3 obtained from the experimental tensor of the O_3^- was 7.86 mT. Assuming a value of $A_1 \approx A_2 \approx 0$ mT for the hyperfine constant along g_1 and g_2, the isotopic and anisotropic part of the hyperfine interaction

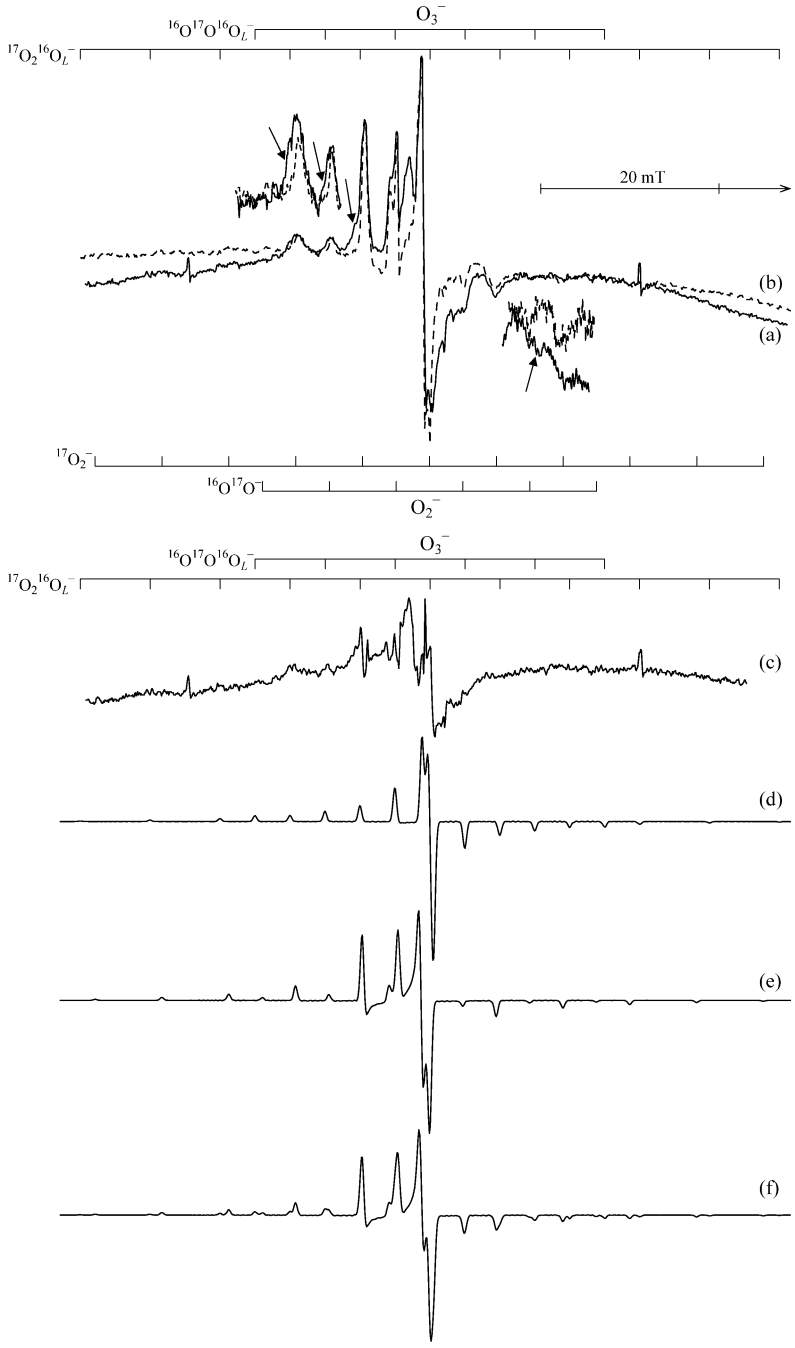

Fig. 2. Observed (a,b) and simulated (d,e,f) ESR spectra of the oxygen radical species on the TiO_2–SiO_2 sample at 77 K. (a) After UV irradiation at 77 K in the presence of ^{17}O-enriched oxygen (1.0 Torr) (solid line), (b) followed by warming the samples to room temperature (dotted line), (c) the spectrum subtracting (b) from (a). The four arrows show the parts where the difference between (a) and (b) are obviously observed. The simulated spectra are for (d) O_3^-, (e) O_2^-, and (f) a sum of O_3^- and O_2^- with the O_3^-/O_2^- ratio of 0.58. The following parameters are employed for the simulation of O_3^- ($g_1 = 2.0080$, $g_2 = 2.0030$, $g_3 = 2.0026$, $A_1 = A_2 = 0$ mT, $A_3 = 7.86$ mT), and O_2^- ($g_{xx} = 2.0025$, $g_{yy} = 2.0090$, $g_{zz} = 2.0250$, $A_{xx} = 7.51$ mT, $A_{yy} = A_{zz} = 0$ mT).

were calculated in the following manner:

$$a_{\text{iso}} = \tfrac{1}{3} \times (7.86 + 0 + 0) = 2.62 \text{ mT}, \tag{2}$$

$$\begin{vmatrix} 0 & & \\ & 0 & \\ & & 7.86 \end{vmatrix} = 2.62 + \begin{vmatrix} -2.62 & & \\ & -2.62 & \\ & & 5.24 \end{vmatrix}. \tag{3}$$

Here a_{iso} and 2β are 2.62 and 5.24 mT, respectively.

To calculate the spin densities in the $2s$ and $2p$ orbitals, one may compare a_{iso} and 2β with the theoretical values obtained for the odd spin, completely in either a $2s$ or a $2p$ orbital, which are denoted by A_0 and B_0, respectively. The spin densities in the above orbitals are a_{2s}^2 and C^2. The two components can then be expressed as

$$a_{\text{iso}} = a_{2s}^2 A_0, \tag{4}$$

$$2\beta = C^2 B_0. \quad (5)$$

Using the theoretical values of $A_0 = -166.0$ mT and $B_0 = 10.4$ mT of ^{17}O [58], we determined the spin densities in the $2s$ and $2p_z$ orbitals to be 0.016 and 0.51, respectively. Therefore, the total spin density on two oxygen nuclei of molecular oxygen was estimated to be 1.02. This spin density is just an approximate value due to the unobserved hyperfine constants along g_1 and g_2. However, it is strongly suggested that the spin density on the lattice oxygen in the T-type O_3^- is very small, and the free electron is largely localized on the two oxygen nuclei originating from the O_2 molecule in the following form, similar to the O_3^- generated on reduced V_2O_5/SiO_2 without photoirradiation [60]

This means that the photoformed hole on lattice oxygen is transferred to an adsorbed O_2 molecule upon the formation of the O_3^-. It could also be said that an O_2 molecule accepts the hole on the lattice oxygen to produce adsorbed O_2^+-like species

$$O_L^- + O_2 \rightarrow O_3^- \left(O_L^{2-} \text{ (electronic neutral)} + O_2^+\right). \quad (6)$$

4. Discussion

4.1. Why does the photoformed O_3^- on TiO_2–SiO_2 promote the epoxidation?

As previously reported, the O_3^- is generated by the reaction between the photoformed hole center on the lattice oxygen (O_L^-) and molecular oxygen, as shown in Eq. (6). The photoepoxidation of various alkenes proved that the O_3^- has the electrophilic property (Table 1). ESR with ^{17}O-enriched oxygen demonstrated that the hole in O_3^- is localized not on the moiety originating from the lattice oxygen but on the moiety originating from the O_2 molecule (Fig. 2). The photoepoxidation of propene with $^{18}O_2$ showed that the oxygen atom derived from the O_2 molecule is inserted into propene to produce PO (Table 4). These results suggest that the O_L^- attracts the electron into the O_2 molecule to form O_3^-, the oxygen atoms derived from molecular oxygen in the O_3^- assume an electron-deficient state like O_2^+, and one of the atoms electrophilically attacks the C=C bond in alkene to produce epoxide. The O_3^- could yield the electrophilic atomic oxygen, which could be why the O_3^- promotes the epoxidation.

In the photoepoxidation of various alkenes, epoxides were formed nonstereospecifically (Tables 1–3). This suggests that the photoepoxidation proceeds through the biradical-like intermediate in a manner similar to that of the epoxidation with $O(^3P)$ [39–41], UV-irradiated NO_2 [48–50], and vanadium hydroperoxo species [51]. The O_3^- might add a radical atomic oxygen species, such as $O(^3P)$, to produce epoxide.

4.2. Reaction mechanism of photooxidation of propene

In the previous study, the reaction mechanism for the production of PO and other molecules was proposed [24]. In addition, from the results of the present study, the following were clarified: (1) The oxygen atoms derived from molecular oxygen in the O_3^- are in an electron-deficient state (Fig. 2). (2) The oxygen atom in PO, which is donated by the O_3^-, originates from molecular oxygen (Table 4). (3) The production of ethanal and acrolein involves the oxidation of propene by both the lattice oxygen and molecular oxygen (Table 4).

Thus, the previously proposed reaction mechanism could be improved as shown in Scheme 1. When the isolated tetrahedral Ti species (species **I**) absorbs UV light ($\lambda < 250$ nm), LMCT from O to Ti occurs on the $[Ti^{4+}–O_L^{2-}]$ moiety, and the excited $[Ti^{3+}–O_L^-]^*$ is formed (species **II**). The photoformed O_L^- and Ti^{3+} react with O_2 to produce O_3^- and O_2^-, respectively (species **III**). In this moment, the hole exists on the O atom derived from molecular oxygen in the O_3^-, which can be also described as O_L^{2-} and O_2^+, and then the electron-deficient oxygen atom electrophilically reacts with propene (species **IV**) to produce PO. It was not confirmed how the residual oxygen atom in the O_3^- would be consumed after the formation of PO. However, the selectivity for PO over the TiO_2–SiO_2 reached 60% when route A and route B proceeded in parallel. The residual oxygen atom derived from the O_2 molecule in the O_3^- should be employed with the formation of one more PO, and the hole would move back to the lattice oxygen. In this scheme, the O_2^- seems not to be involved in the epoxidation mechanism. However, the O_2^- attracts the electron on the Ti^{3+} and results in the separation of electron density. If the O_2^- did not exist, the electron on the Ti^{3+} should immediately combine with the hole on the lattice oxygen, and the O_3^- should not be so stable. It is well known that O_2^- is a very stable oxygen species [56]. The O_2^- signal on the TiO_2–SiO_2 samples did not disappear, even in the presence of propene and O_2 at room temperature [24], but the signal intensity gradually decreased in a few days. If the O_2^- existed on the isolated tetrahedral Ti site after the O_3^- was consumed to produce PO, the epoxidation should not cycle catalytically and the TON (produced PO/Ti atoms) should not exceed 2. However, the TON reached 2.8 over the TiO_2/SiO_2 0.1 mol% when PO underwent the consecutive reactions [25]. Therefore, the O_2^- would be eliminated as an O_2 molecule, and the electron should recombine with the hole on the lattice oxygen to produce initial $[Ti^{4+}–O_L^{2-}]$ (species **I**), although the elimination rate of the O_2^- might be slow.

On the other hand, when O_L^- reacts directly with propene, allyl radical (species **VI**) or methyl radical (species **VII**) is formed through H abstraction or CC bond fission. In the case of species **VI**, allyl radical, abstracted H atom, lattice oxygen O_L, and one oxygen atom of O_2^- should form an activated complex to produce acrolein and H_2O. The lattice oxygen and one oxygen atom of O_2^- would be inserted

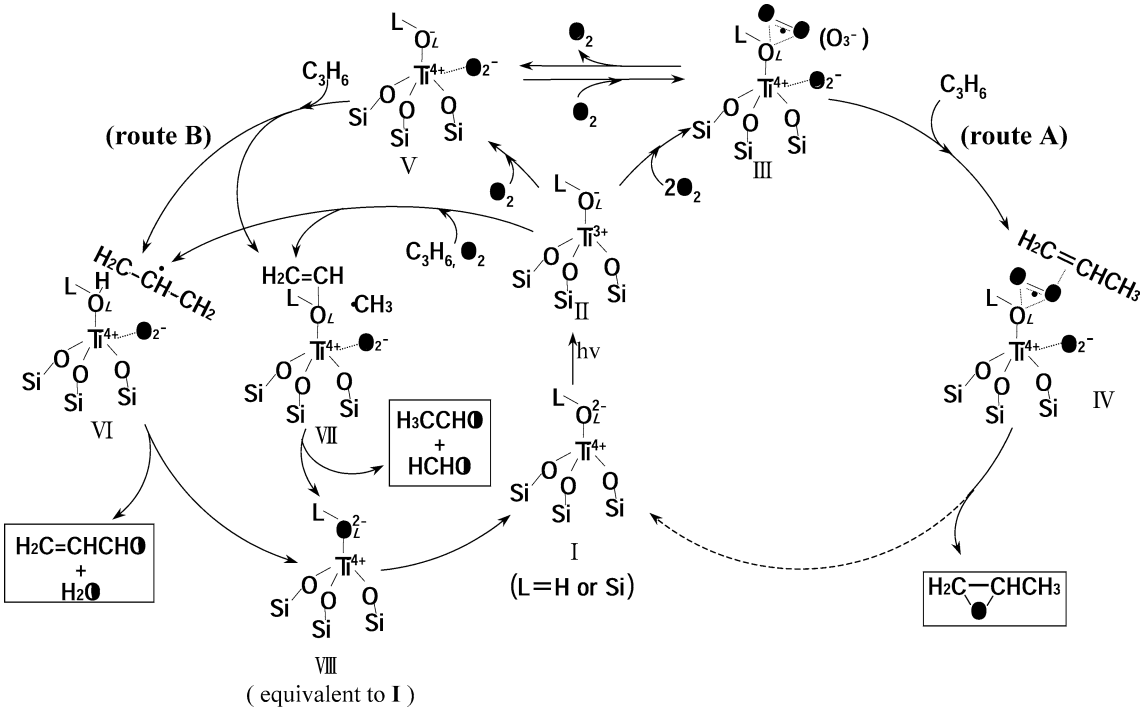

Scheme 1. Proposed mechanism for the formation of PO, ethanal and acrolein over the isolated tetrahedral Ti species in the photooxidation of propene. The black and normal oxygen atoms are originated from O_2 molecule and lattice oxygen, respectively.

into acrolein or H_2O equally, and the debris of O_2^- would be incorporated into the lattice. Therefore, approximately half of the acrolein contained oxygen atoms derived from molecular oxygen. In species **VII**, methyl radical and CH_2CH intermediate should react with O_L and one oxygen atom of O_2^- in a manner similar to that of species **VI**.

Anpo et al. previously reported the quantum chemical studies of photogenerated O_3^- on porous Vycol glass (PVG) [53]. The quantum chemical calculation showed that the formation of O_3^- resulted in weakening and extension of the OO bond in the O_2 molecule. Also in the present system of the TiO_2–SiO_2 sample, the OO bond of molecular oxygen in the O_3^- would be weakened when the electron density in the bonding orbital is reduced by electron donation to the lattice oxygen, and the atomic-like oxygen species should be added to the C=C bond in alkene.

4.3. *Photoformed* O_3^- *on the various metal oxides*

The O_3^- species were observed on several UV-irradiated metal oxides [56], such as TiO_2 [61,62], ZnO [63], MgO [64], and PVG [53]. However, there are no reports that PO was formed as a main product on these oxides.

The O_3^- on TiO_2 [61,62], ZnO [63], and MgO [64], exhibited orthorhombic *g* values. The shape of the O_3^- is different from that in the present case. Therefore, the nature of the O_3^- on the TiO_2–SiO_2 will be different from these systems. On the other hand, the O_3^- on PVG [53] is the T-shape O_3^- similar to that on the TiO_2–SiO_2. However, PVG did not produce epoxides in the photoepoxidation of olefins [65]. It is assumed that not only the formation of the O_3^-, the moderate stability of the O_3^- and selective reaction of O_L^- to O_2 would determine the production of epoxides. In the presence of O_2 and olefin, the O_L^- on TiO_2–SiO_2 should preferably react with O_2 to produce O_3^- yielding epoxides, but the O_L^- on PVG might preferably react with olefin to produce C=C cleavage products. Whether the O_3^- could react with propene before decomposition would also be important. It is speculated that the electronic properties of the photoexcited center in silica (for example, Ti in TiO_2–SiO_2) influences these factors. In addition, PVG is a porous silica material containing some impurities such as B_2O_3 (2.95 wt%), Na_2O (0.04 wt%), Al_2O_3 (2.95 wt%), and ZrO_2 (0.72 wt%), and it is expected to have acid sites. As shown in our previous study [27], the acidity on PVG should convert PO to other products and should inhibit epoxide production.

5. Conclusion

The photoformed hole center on the lattice oxygen (O_L^-) over the TiO_2–SiO_2 catalyst attracts an electron from an O_2 molecule to form the electrophilic O_3^-. The oxygen atom moiety derived from molecular oxygen in the O_3^- enters an electron-deficient state (the O_3^- would also be described as O_L^{2-} (electronic neutral) and adsorbed O_2^+) and electrophilically attacks C=C bond in alkene to produce epoxide. This paper showed for the first time that the T-shape O_3^- has an electrophilic property effective for the epoxidation of alkenes with allylic C–H bonds.

Acknowledgments

We thank Prof. Y. Okamoto, Prof. J. Kumagai, Dr. Y. Isobe (Department of Applied Chemistry, Graduate School of Engineering, Nagoya University), Mr. Y. Nagara, and Mr. M. Kawahara (Japan Chemical Innovation Institute, Nagoya) for their help in ESR measurement.

This work was supported by a grant-in-aid from the Japanese Ministry of Education, Science, Art, Sports and Culture, and by the Nippon Sheet Glass Foundation for Materials Science and Engineering.

References

[1] B.K. Hoenett, Heterogeneous Catalytic Oxidation, Willey, Chichester, 2000.
[2] G. Centi, F. Cavani, F. Trifrò, Selective Oxidation by Heterogeneous Catalysis, Kluwer-Academic–Plenum, New York, 2001.
[3] J.R. Monnier, Appl. Catal. A 221 (2001) 73, and references therein.
[4] G. Lu, X. Zuo, Catal. Lett. 58 (1999) 67.
[5] T. Miyaji, P. Wu, T. Tatsumi, Catal. Today 71 (2001) 169.
[6] K. Murata, Y. Kiyozumi, Chem. Commun. (2001) 1356.
[7] J. Lu, M. Luo, H. Lei, C. Li, Appl. Catal. A 237 (2002) 11.
[8] J. Lu, M. Luo, H. Lei, X. Bao, C. Li, J. Catal. 211 (2002) 552.
[9] K. Murata, Y. Liu, N. Mimura, M. Inaba, J. Catal. 220 (2003) 513.
[10] Y. Liu, K. Murata, M. Inaba, Catal. Lett. 93 (2004) 109.
[11] T. Hayashi, L.B. Han, S. Tsubota, M. Haruta, Ind. Eng. Chem. Res. 34 (1995) 2298.
[12] T.A. Nijhuis, S. Musch, M. Makkee, J.A. Moulijn, Appl. Catal. A 196 (2000) 217.
[13] A. Maldotti, A. Molinari, R. Amadelli, Chem. Rev. 102 (2002) 3811.
[14] Y. Kanno, T. Oguchi, H. Sakuragi, K. Tokumaru, Tetrahedron Lett. 21 (1980) 467.
[15] M.A. Fox, C. Chen, J. Am. Chem. Soc. 103 (1981) 6757.
[16] T. Ohno, K. Nakabeya, M. Matsumura, J. Catal. 176 (1995) 76.
[17] Y. Matsuda, S. Sakamoto, H. Koshima, Y. Murakami, J. Am. Chem. Soc. 107 (1985) 6415.
[18] L. Weber, I. Imiolczyk, G. Haufe, D. Rehorek, H. Hennig, J. Chem. Soc., Chem. Commun. (1991) 301.
[19] L. Weber, R. Hommel, J. Behling, G. Haufe, H. Hennig, J. Am. Chem. Soc. 116 (1994) 2400.
[20] P. Pichat, J. Herrmann, J. Disdier, M. Mozzanega, J. Phys. Chem. 83 (1979) 3122.
[21] F. Blatter, H. Sun, H. Frei, Catal. Lett. 35 (1995) 1.
[22] F. Blatter, H. Sun, S. Vasenkov, H. Frei, Catal. Today 41 (1998) 297.
[23] Y. Xiang, S.C. Larsen, V.H. Grassian, J. Am. Chem. Soc. 121 (1999) 5063.
[24] C. Murata, H. Yoshida, J. Kumagai, T. Hattori, J. Phys. Chem. B 107 (2003) 4364.
[25] H. Yoshida, C. Murata, T. Hattori, Chem. Commun. (1999) 1551.
[26] C. Murata, H. Yoshida, T. Hattori, Stud. Surf. Sci. Catal. 143 (2002) 845.
[27] H. Yoshida, C. Murata, T. Hattori, J. Catal. 194 (2000) 364.
[28] T. Tanaka, H. Nojima, H. Yoshida, H. Nakagawa, T. Funabiki, S. Yoshida, Catal. Today 16 (1993) 297.
[29] H. Yoshida, T. Tanaka, M. Yamamoto, T. Yoshida, T. Funabiki, S. Yoshida, J. Catal. 171 (1997) 351.
[30] H. Yoshida, T. Tanaka, M. Yamamoto, T. Funabiki, S. Yoshida, Chem. Commun. (1996) 2125.
[31] H. Yoshida, T. Tanaka, M. Yamamoto, T. Yoshida, T. Funabiki, S. Yoshida, J. Catal. 171 (1997) 351.
[32] H. Yoshida, C. Murata, T. Hattori, Chem. Lett. (1999) 901.
[33] H. Yoshida, T. Shimizu, C. Murata, T. Hattori, J. Catal. 220 (2003) 226.
[34] C. Murata, H. Yoshida, T. Hattori, Chem. Commun. (2001) 2412.
[35] F. Amano, T. Tanaka, T. Funabiki, Langmuir 20 (2004) 4236.
[36] H. Yoshida, Curr. Opin. Solid State Mater. Sci. 7 (2003) 435.
[37] Y. Moro-oka, M. Akita, Catal. Today 41 (1998) 327.
[38] Y. Moro-oka, Catal. Today 45 (1998) 3.
[39] R.J. Cvetanović, Adv. Photochem. 1 (1963) 115, and references therein.
[40] R.J. Cvetanović, J. Chem. Phys. 30 (1959) 19.
[41] S. Hirokami, R.J. Cvetanović, J. Am. Chem. Soc. 96 (1974) 3738.
[42] R.A. Sheldon, H. Bekkum, Fine Chemicals through Heterogeneous Catalysis, Willey–VCH, Weinheim, 2001.
[43] R. Sheldon, in: Aspects of Homogeneous Catalysis, vol. 4, Weinheim, Reidel, 1981, pp. 3–70.
[44] M.G. Clerici, G. Bellussi, U. Romano, J. Catal. 129 (1991) 159.
[45] B. Notari, Adv. Catal. 41 (1996) 253.
[46] B.J. Wallar, J.D. Lipscomb, Chem. Rev. 96 (1996) 2625.
[47] R. Lange, J. Hekkink, K. Keizer, A. Burggraaf, J. Noncryst. Solids 191 (1995) 1.
[48] M. Nakata, H. Frei, J. Am. Chem. Soc. 111 (1989) 5270.
[49] M. Nakata, H. Frei, J. Phys. Chem. 94 (1990) 5270.
[50] D.J. Fitzmaurice, H. Frei, J. Phys. Chem. 96 (1992) 10308.
[51] H. Minoun, L. Saussine, E. Daire, M. Postel, J. Fischer, R. Weiss, J. Am. Chem. Soc. 105 (1983) 3101.
[52] H. Courbon, M. Formenti, P. Pichat, J. Phys. Chem. 81 (1977) 550.
[53] M. Anpo, Y. Kubokawa, T. Fuji, S. Suzuki, J. Phys. Chem. 88 (1984) 2572.
[54] M. Shiotani, G. Moro, J.H. Freed, J. Phys. Chem. 74 (1981) 2616.
[55] M. Anpo, N. Aikawa, Y. Kubokawa, M. Che, C. Louis, E. Giamello, J. Phys. Chem. 89 (1985) 5689.
[56] M. Che, A. Tench, J., Adv. Catal. 32 (1983) 1, and references therein.
[57] V.V. Nikisha, B.N. Shelimov, V.B. Kazansky, Kinet. Katal. 15 (1974) 676.
[58] J.H. Lunsford, Adv. Catal. 22 (1972) 265.
[59] N.-B. Wong, J.H. Lunsford, J. Chem. Phys. 55 (1971) 3007.
[60] B.N. Shelimov, C. Naccache, M. Che, J. Catal. 37 (1975) 279.
[61] A.R. Gonzalez-Elipe, G. Munuera, J. Soria, J. Chem. Soc., Chem. Farady Trans. I 75 (1979) 736.
[62] P. Meriaudeau, J.C. Vedrine, J. Chem. Soc., Chem. Farady Trans. I 78 (1982) 1297.
[63] K.M. Sancier, T. Freud, J. Catal. 3 (1964) 293.
[64] M. Iwamoto, J.H. Lunsford, Chem. Phys. Lett. 66 (1979) 48.
[65] Y. Kubokawa, M. Anpo, C. Yun, in: Proceedings of the 7th International Congress on Catalysis, Elsevier, 1980, p. 1170.